Received: 31 October 2022 | Revised: 9 March 2023 | Accepted: 17 March 2023

DOI: 10.1111/jre.13123

Journal of PERIODONTAL RESEARCH WILEY

ORIGINAL ARTICLE

Effects of prolonged stimulation with heated tobacco products (Ploom TECH$^+$) on gingival epithelial cells

Osamu Uehara[1,2] | Norihiro Nakamoto[3] | Daichi Hiraki[4] | Durga Paudel[2] | Nodoka Sugiyama[3] | Tetsuro Morikawa[5] | Koki Yoshida[2,5] | Yutaka Kawano[2,6] | Tsuyoshi Shimo[4] | Yasushi Furuichi[2,3] | Hiroko Miura[1] | Yoshihiro Abiko[2,5]

[1]Division of Disease Control and Molecular Epidemiology, Department of Oral Growth and Development, School of Dentistry, Health Sciences University of Hokkaido, 1757 Kanazawa, Ishikari-Tobetsu, 061-0293, Japan

[2]Advanced Research Promotion Center, Health Sciences University of Hokkaido, 1757 Kanazawa, Ishikari-Tobetsu, 061-0293, Japan

[3]Division of Periodontology and Endodontology, Department of Oral Rehabilitation, School of Dentistry, Health Sciences University of Hokkaido, 1757 Kanazawa, Ishikari-Tobetsu, 061-0293, Japan

[4]Division of Reconstructive Surgery for Oral and Maxillofacial Region, Department of Human Biology and Pathophysiology, School of Dentistry, Health Sciences University of Hokkaido, 1757 Kanazawa, Ishikari-Tobetsu, 061-0293, Japan

[5]Division of Oral Medicine and Pathology, Department of Human Biology and Pathophysiology, School of Dentistry, Health Sciences University of Hokkaido, 1757 Kanazawa, Ishikari-Tobetsu, 061-0293, Japan

[6]Department of Gastroenterology and Oncology, Tokushima University Graduate School of Biomedical Sciences Tokushima, 3-18-15, Kuramoto-cho, Tokushima, 770-8503, Japan

Correspondence
Yoshihiro Abiko, Division of Oral Medicine and Pathology, Department of Human Biology and Pathophysiology, School of Dentistry, Health Sciences University of Hokkaido, 1757 Kanazawa, Ishikari-Tobetsu, Hokkaido 061-0293, Japan.
Email: yoshi-ab@hoku-iryo-u.ac.jp

Abstract

Objective and Background: Heated tobacco products have recently become commercially available. These products, as well as combustible cigarettes, produce aerosols; the risk of various diseases associated with heated tobacco products may be the same or higher than that with combustible cigarettes. In this study, we examined the effect of Ploom TECH$^+$ extract on gingival epithelial cells.

Methods: Tobacco leaves from Ploom TECH$^+$ tobacco capsules and water were mixed and heated; the supernatant subsequently collected was the heated tobacco product (HTP; control: HTP not added). Normal human gingival epithelial progenitors were cultured alternately with or without HTP for a total of 1 month. Subsequently, RNA, DNA, and proteins were isolated from these samples and comprehensively analyzed using RNA sequencing (RNA-seq), reduced representation bisulfite sequencing (RRBS), and western blotting, respectively.

Results: RNA-seq revealed that 284 genes showed a twofold increase and 145 genes showed a twofold decrease in gene expression. A heat map showed genetic differences between the control and HTP groups. A principal component analysis plot showed a clear genetic distribution between the control and HTP. Gene Ontology (GO) analysis showed that genes related to seven GO terms, including cornification and keratinization, were induced by long-term HTP stimulation. By contrast, GO pathways with a significant decrease in component expression were not detected. RRBS revealed that CpG island methylation increased more than twofold in 158 genes and decreased to less than twofold in 171 genes. Methylation of these CpG islands was not correlated with changes in gene expression levels. HTP treatment increased S100A7 expression.

Conclusion: Long-term HTP stimulation affected epithelial differentiation and keratinization of gingival epithelial cells. Thus, habitual use of Ploom TECH$^+$ may be a risk factor for tobacco-related oral mucosal diseases.

KEYWORDS
DNA methylation, gingival epithelial cell, heated tobacco product, reduced representation bisulfite sequencing, RNA sequencing

Osamu Uehara and Norihiro Nakamoto contributed equally to the work.

1 | INTRODUCTION

Consumption of combustible cigarettes lead to systemic issues such as the development of cancer, cardiovascular disease, and respiratory illness. Cigarettes are important risk factors for oral cancer and periodontal disease, which is of concern for dental professionals.[1] Smoking cigarettes, which contain approximately 70 types of carcinogens and other harmful chemicals, often causes genetic and epigenetic alterations leading to oral cancer and induces abnormal blood circulation leading to periodontal diseases.

Recently, heated tobacco products, which do not require combustion, have become commercially available. These products can be broadly divided into two types: "high-temperature heating" type, wherein tobacco leaves are heated at 200–350°C and "low-temperature heating" type, wherein tobacco leaves are heated at 30–40°C. IQOS is a high-temperature heating-type cigarette that generates steam by directly heating tobacco leaves in a heater. Ploom TECH$^+$ is a low-temperature heating-type cigarette that vaporizes the liquid. Although many studies have reported on the risks associated with the high-temperature type, to the best of our knowledge,[2] no reliable independent data on the risks associated with the low-temperature type have been reported thus far. Heated tobacco products were initially considered less toxic than combustible cigarettes; however, an increasing number of studies have reported toxicity.[3,4] The risk of carcinogenesis owing to heated tobacco might be the same or higher than that of combustible cigarettes.[5] Several clinical cases of fulminant pneumonia possibly attributable to the use of heated tobacco have been reported.[6] An in vitro experiment showed that the components of this type of tobacco directly damaged bronchial epithelial cells and vascular endothelial cells.[7]

To the best of our knowledge, the effect of heated tobacco products on oral mucosa has not yet been shown. Heated tobacco contains many toxic substances, although to a significantly lesser degree than that in combustible cigarettes, and its use may increase the risk of oral cancer and periodontal diseases. Oral epithelium exposed to heated tobacco may experience pathological changes leading to the development of oral cancer and periodontal disease. We hypothesized that heated tobacco products induce molecular changes in the oral epithelium. Therefore, in this study, we examined the effect of Ploom TECH$^+$ extract on gingival epithelial cells. The oral mucosa of individuals who use heated tobacco products is regularly exposed to the tobacco for a long time. The cells derived from oral mucosa should be stimulated for a long time. The cells are usually stimulated with the chemical substances for 1 to 72 h in vitro since the cells have to be fed by medium every 72 h. These stimulation periods may be too short to observe the effect of the heated tobacco on the cells. We previously developed an in vitro model to stimulate cells for 1 month as a long-term and chronic stimulation.[8] Therefore, we subjected oral epithelial cells to prolonged stimulation using our previous model.

2 | MATERIAL AND METHODS

2.1 | Cell culture

Human gingival epithelial progenitors (HGEPs) were purchased from CELLnTEC Advanced Cell Systems (Basel, Switzerland) and cultured in CnT-Prime epithelial culture medium (CELLnTEC Advanced Cell Systems) at 37°C in a humidified atmosphere of 95% air and 5% CO_2. HEGPs were kept in the medium not to be differentiated.

2.2 | Heated tobacco product (HTP) preparation

Ploom TECH$^+$ (Japan Tobacco Inc.) tobacco capsules were disassembled, and the tobacco leaves in the capsules were collected in 1.5-mL tubes. Next, the leaves were weighed, and 3 mL water was added per gram of tobacco leaves. Subsequently, the mixture was heated at 60°C for 120 min.[9] Thereafter, the tobacco leaves and supernatant were separated using centrifugation at 15,000 rpm for 15 min, and the supernatant was collected and used as the extract (HTP).[9]

2.3 | Cell viability assays

Cell viability was determined using the cell proliferation reagent water-soluble tetrazolium salt (WST-1; Thermo Fisher Scientific). The HGEPs were seeded in 96-well plates (AGC TECHNO GLASS) in the culture medium and cultured overnight. The cells were treated with different concentrations of HTP (0%, 0.1%, 0.2%, 0.5%, 1%, 2%, 5%, and 10%); 0% HTP samples were used as controls. Subsequently, the plates were incubated for 24, 48, and 72 h, following which 10 μL WST-1 was added to each well and the cells were cultured for 1 h. Absorbance was measured at 450 nm using the Multiskan FC system (Thermo Fisher Scientific). The experiment was repeated six times. Statistical analysis was performed using SPSS version 26 (SPSS, Inc.). Results were compared using the Kruskal–Wallis test, with a p-value of $<.05$ being considered statistically significant.

2.4 | Sample preparation

The HGEPs were seeded in 6-well plates (AGC TECHNO GLASS) at a density of 3.0×10^5 cells/well in a culture medium and cultured overnight. The HGEPs were treated with 1% HTP. The culture medium was replaced every 3 days while alternating with and without HTP for a total of 1 month.[8] Untreated samples were used as controls. The same amount of water as HTP was added to the controls every 3 days. Genomic DNA was extracted using the DNeasy Blood & Tissue Kit (Qiagen, Hilden), according to the manufacturer's instructions. DNA extracts were stored at −20°C until use in experiments and were utilized for bisulfite processing. Total RNA was extracted from HGEPs using the TRIzol Reagent

(Thermo Fisher Scientific) and purified using the RNeasy Mini kit (Qiagen GmbH, Hilden) according to the manufacturers' protocols. RNA extracts were stored at −80°C and used for reverse transcription. Total protein was extracted from the HGEPs using the EzRIPA lysis kit (ATTO) according to the manufacturer's instructions. Protein extracts were stored at −80°C until use and were utilized for western blot analysis. The experiment was repeated three times for RNA sequencing (RNA-seq) and reduced representation bisulfite sequencing (RRBS) and six times for quantitative reverse transcriptase PCR, quantitative methylation-specific PCR (qMSP), and western blotting.

2.5 | RNA-seq and functional enrichment analysis

Samples were run on a BioAnalyzer to assess total RNA integrity. Only high-quality RNA samples (RNA integrity number ≥9.0) were used to construct the sequence library. PCR-based amplification was performed using the template prepared with the strand-specific library preparation method (dUTP method) and an index sequence-containing primer to prepare a sequence library (NEBNext Poly(A) mRNA Magnetic Isolation Module; NEBNext Ultra II Directional RNA Library Prep Kit for Illumina). RNA-seq data were obtained using the NovaSeq 6000 system (Illumina). The sequence reads were trimmed using Trimmomatic (ver.0.38). Trimmed sequence reads were mapped to the reference genome (hg38) using HISAT2 (ver.2.1.0). The raw read count for each gene was calculated using featureCounts (ver.1.6.3). The raw read count was uploaded to iDEP.95 (http://bioinformatics.sdstate.edu/idep95/) for hierarchical clustering, principal component analysis (PCA), correlation evaluation, heat map creation, and functional enrichment analysis.[10] Initial settings of iDEP were used for the analysis.

2.6 | Quantitative reverse transcriptase PCR

The extracted RNA (2 μg) was reverse-transcribed to cDNA using the ReverTra Ace® qPCR RT Master Mix (TOYOBO). mRNA expression levels were measured using a LightCycler®96 system (Roche Diagnostics, Basel, Switzerland). Table 1 lists the primer sequences used in this study. Real-time PCR was performed using the obtained cDNA, KAPA SYBR FAST qPCR Mix (Kapa Biosystems), and a pair of primers, according to the manufacturers' protocols. The PCR program was as follows: pre-incubation at 95°C for 3 min; denaturation at 95°C; and 40 cycles each of denaturation at 95°C for 10 s, annealing at 60°C for 20 s, and elongation at 72°C for 1 s. The relative mRNA expression levels were calculated in terms of the Cq value (value obtained by subtracting the Cq value of GAPDH mRNA from the Cq value of the target mRNA) using the ΔΔCq method.[11] Specifically, the amount of target mRNA relative to GAPDH mRNA was expressed as $2^{-(\Delta Cq)}$. Data have been expressed in terms of the ratio of the target mRNA to GAPDH mRNA. Results were compared using the Mann–Whitney *U* test, with a *p*-value of <.05 being considered statistically significant.

TABLE 1 Primer sequences used for quantitative reverse transcriptase PCR and quantitative methylation-specific PCR.

Gene	Sequence (5′–3′)
GAPDH-F	GTGAAGGTCGGAGTCAAC
GAPDH-R	GTTGAGGTCAATGAAGGG
KRT13-F	CCAGGACGCCAAGATGATTG
KRT13-R	CGACCAGAGGCATTAGAGGT
KLK12-F	CCTGTGGACAAGATGGCATC
KLK12-R	AAGGGCTGGCAGGAGTTAAA
S100A7-F	GCACAAATTACCTCGCCGAT
S100A7-R	ATGGCTCTGCTTGTGGTAGT
KRT13-MF	TCGTTTTATTAGAAAGCGGG
KRT13-MR	ATAACGATCTCCTACTCCAAACGTA
KRT13-UF	TGTTTTATTAGAAAGTGGGG
KRT13-UR	AATAACAATCTCCTACTCCAAACATA
KLK12-MF	GATTGGATCGAGTAGATTCGGTA
KLK12-MR	TACCCCAACCTAAAACGTAA
KLK12-UF	TGGATTGAGTAGATTTGGTA
KLK12-UR	ATAATACCCCAACCTAAAACATAA
S100A7-MF	AGTTAAGGTGGGGTTTACGGT
S100A7-MR	CTCCAACTTCACAATCGAAA
S100A7-UF	GAGTTAAGGTGGGGTTTATGGT
S100A7-UR	CTCCAACTTCACAATCAAAA

Abbreviations: F, forward; R, reverse; M, methylated; U, unmethylated.

2.7 | Western blot analysis

Thirty micrograms of protein was used for western blot analysis. Pre-cast gels (5%–20% gradient polyacrylamide gels; e-PAGEL, ATTO) were used for sodium dodecyl sulfate–polyacrylamide gel electrophoresis. The separated protein bands were transferred onto a polyvinylidene fluoride transfer membrane (ATTO). Blocking was performed using Tris-buffered saline (TBS) containing 5% skimmed milk for 1 h at 20°C. The primary antibodies used were polyclonal rabbit anti-cytokeratin 13 (1:1000; Proteintech Group), polyclonal rabbit anti-kallikrein 12 (1:1000; Thermo Fisher Scientific), polyclonal rabbit anti-S100A7 (1:1000; Proteintech Group), and monoclonal mouse anti-GAPDH (1:10000; Proteintech Group) antibodies. The membranes were incubated with each primary antibody overnight at 4°C, washed three times with TBS containing 0.05% Tween-20, and further incubated with secondary antibodies for 1 h at 20°C. The secondary antibodies used were horseradish peroxidase (HRP)-conjugated goat anti-rabbit IgG (1:10000, Proteintech Group) and HRP-conjugated goat anti-mouse IgG (1:10000, Proteintech Group)

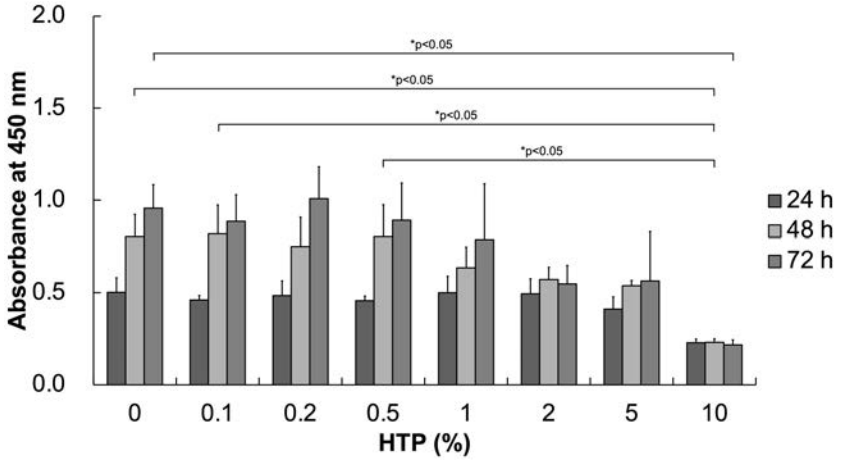

FIGURE 1 Cell viability assays. Cell counts and viability were estimated by performing water-soluble tetrazolium salt (WST-1) assays at 24, 48, and 72 h with different heated tobacco product (HTP) concentrations. Cell viability showed a time-dependent increase with the use of up to 5% HTP. At 24, 48, and 72 h, cell viability did not significantly differ at the same time point between any HTP and the control. Cell viability was significantly lower with ≥10% HTP than in the control. Data are presented as mean ± SD, with a *p*-value of <.05 indicating significance.

antibodies. Cytokeratin 13 (KRT13), kallikrein 12 (KLK12), S100A7, and GAPDH bands were visualized using an enhanced chemiluminescence system (Clarity Western ECL substrate; Bio-Rad) and WSE-6100 LuminoGraph I (ATTO). Intensities of KRT13, S100A7, and GAPDH were recorded using the ImageSaver6 software (ATTO), and the bands were quantified using the image analysis software CS Analyzer 4 (ATTO). The ratios of intensity of KRT13, S100A7, and GAPDH in HTP-treated (HTP) or untreated (control) HGEPs from two independent experiments were calculated. Results were compared using the Mann–Whitney *U* test, with a *p*-value of <.05 being considered statistically significant.

2.8 | Quantitative methylation-specific PCR

Samples were run on a BioAnalyzer to assess total DNA integrity. Only high-quality DNA samples (DNA integrity number ≥9.0) were used to construct the sequence library. The extracted DNA was treated with sodium bisulfite using the EpiTect Plus Bisulfite Kit (Qiagen). DNA methylation of *KRT13*, *KLK12*, and *S100A7* was analyzed using SYBR Green–based qMSP. Two sets of PCR primers were designed using the MethPrimer program (http://www.urogene.org/methprimer/). Methylated and unmethylated primers were designed targeting the promoters (Table 1). The PCR mixture (20 μL) comprised 1.0 μL bisulfite-treated DNA template, 10 μL KAPA SYBR FAST qPCR Mix, and a pair of primers. DNA methylation was analyzed using the LightCycler®96 system. The PCR program was as follows: pre-incubation at 95°C for 3 min; denaturation at 95°C; and 50 cycles each of denaturation at 95°C for 10 s, annealing at 60°C for 20 s, and elongation at 72°C for 1 s. The DNA methylation percentage in the samples was estimated using the following formula: DNA methylation $(\%) = M/(M+U) \times 100 = 1/(1+U/M) \times 100 = 1/(1+2^{(-\Delta Cq)}) \times 100$, where *M* is the copy number of the methylated gene, *U* is the copy number of the unmethylated gene, and $\Delta Cq = Cq_U - Cq_M$.[12] Results were compared using the Mann–Whitney *U* test, with a *p*-value of <.05 being considered statistically significant.

2.9 | Reduced representation bisulfite sequencing

The samples were run on a BioAnalyzer to assess genomic DNA integrity. Only high-quality DNA samples (DNA integrity number ≥9.0) were used to construct the sequence library. To perform methylation analysis of the CpG region, the CpG-rich region was enriched by cutting genomic DNA with the restriction enzyme MspI, adding a TruSeq adapter, performing bisulfite treatment, and adding an index sequence. The RRBS library was prepared using the Zymo Research Zymo-Seq RRBS Library Kit (Zymo Research). RRBS data were obtained using the NovaSeq 6000 system (Illumina). Sequence reads were trimmed using Trim Galore (ver.0.5.0). Trimmed sequence reads were mapped to the reference genome using Bismark (ver.0.20.0). The methylation rate was calculated, and comparison analysis was performed using methylKit (ver.1.16.0). A heat map was drawn using the differentially methylated cytosine/differentially methylated region methylation rate using stats (ver.3.6.1) and gplots (ver.3.0.1.1). We examined this correlation further by plotting expression logFC versus methylation (CpG island) logFC for all genes using the method described by Chen et al.[13]

3 | RESULTS

3.1 | Cell viability

To determine appropriate experimental conditions for analyzing cell viability maintenance in HTP-stimulated cells, we analyzed cell viability while using different HTP concentrations. Using the WST-1 assay, cell viability was estimated at 24, 48, and 72 h with different HTP concentrations. At 24, 48, and 72 h, cell viability did not significantly

differ at the same time point between any HTP concentration and the control. Cell viability with ≥10% HTP was significantly lower than that in the control ($p < .05$, Figure 1). Based on these data, culture was repeated under the following conditions: 3 days with 1% HTP alternating with 3 days without HTP, for a total of 1 month.

3.2 | Gene expression profiles

For comprehensive RNA-seq analysis, HGEPs alternately cultured with or without 1% HTP for a total of 1 month were used for RNA extraction. The heat map shows differences between the control and HTP for all genes identified using RNA-seq (Figure 2A). The PCA plot revealed clear differences between the control and HTP (Figure 2B). Among differentially expressed genes (DEGs), 284 showed a greater than twofold increase ($p < .05$, Figure 2A–C, Table 2) and 145 showed a more than twofold decrease ($p < .05$, Figure 2A–C, Table 2). Gene Ontology (GO) analyses included the biological process, cellular component, and molecular function categories. According to the functional enrichment results, only seven biological process terms were significantly enriched in DEGs. GO analysis revealed that long-term HTP stimulation increased the expression of components belonging to the GO pathways cornification (70 upregulated genes, such as *KRT13*, *KLK12*, and *PI3* in descending order; $p < .05$), keratinization (84 upregulated genes, such as *KRT13*, *KLK12*, and *PI3*; $p < .05$), epidermal development (279 upregulated genes, such as *KRT13*, *KLK12*, and *S100A7*; $p < .05$), epidermal cell differentiation (196 upregulated genes, such as *KRT13*, *KLK12*, and *S100A7*; $p < .05$), skin development (248 upregulated genes, such as *KRT13*, *KLK12*, and *S100A7*; $p < .05$), keratinocyte differentiation (155 upregulated genes, such as *KRT13*, *KLK12*, and *S100A7*; $p < .05$), and epithelial cell differentiation (498 upregulated genes, such as *KRT13*, *KLK12*, and S100A7; $p < .05$) (Figure 2D,E). Reproducibility was confirmed for *KRT13* (seven pathways), *KLK12* (seven pathways), and *S100A7* (five pathways), which are related to upregulated GO pathways in the iDEP analysis and are the upregulated DEGs.

To confirm the reliability of the expression profiles generated using the RNA-seq and DEG analyses, qRT-PCR was applied to examine the expression of the upregulated candidate genes (*KRT13*, *KLK12*, and *S100A7*). *KRT13* and *KLK12* were GO-related genes. *S100A7* is associated with epidermal development, epidermal cell differentiation, skin development, keratinocyte differentiation, and epithelial cell differentiation. As expected, the qRT-PCR results basically matched the RNA-seq results, confirming the relationship of *KRT13*, *KLK12*, and *S100A7* with elevated component expression in GO pathways; increased expression was confirmed for all three genes ($p < .05$; Figure 3A–C).

3.3 | Protein expression

HTP treatment increased S100A7 expression levels but did not change the KRT13 and GAPDH expression levels (Figure 3D). KLK12 expression was not detected. The ratios of intensity of KRT13/GAPDH in HGEPs treated with or without 1% HTP were 1.00 ± 0.11 and 0.94 ± 0.06, respectively. No significant difference was observed in the ratio of intensities of KRT13/GAPDH between the control and HTP. The ratios of intensity of S100A7/GAPDH in HGEPs treated with or without 1% HTP were 1.00 ± 0.91 and 13.43 ± 6.83, respectively. The *p*-value for the ratio of intensities of S100A7/GAPDH between HTP-treated and untreated HGEPs was <.05 (Figure 3E,F).

3.4 | DNA methylation

For comprehensive RRBS analysis, HGEPs were alternately cultured with or without 1% HTP for a total of 1 month, followed by DNA extraction. Read counts were normalized using methylKit, and differentially methylated cytosines (DMCs) and differentially methylated regions (DMRs) were extracted through logistic regression. A heatmap was drawn using the methylation rate of DMC/DMR. Heatmap analysis showed that the CpG methylation differed between the control and HTP groups (Figure 4A). CpG regions were classified and annotated as follows. CpG island: A genomic region of 200 bases or more, with a total guanine and cytosine content of 50% or more, and a ratio of the actual frequency of occurrence of CG sequences to the predicted value of ≥0.6. CpG islands accumulate in gene promoter regions and are involved in the promotion or suppression of gene expression.[14] CpG shore: Peripheral part of CGI (approximately 2 kb). The methylation status of CpG island shores is tissue specific. CpG shelf: A region between 2 and 4 kb around CGI. interCpG (interCGI): Regions not classified above. When overlapping with multiple divisions, priority was assigned in the order of CGI, shore, shelf, and inter CpG. A total of 158 genes showed greater than twofold hypermethylation (Table 3) and 171 genes showed greater than twofold hypomethylation (Table 4) in CpG islands. Changes in DNA methylation were not correlated with gene expression levels (Figure 4B). Furthermore, DNA methylation levels did not significantly differ between the control and HTP groups for *S100A7*, *KLK12*, and *KRT13* (Figure 4C–E).

4 | DISCUSSION

In the current study, we comprehensively analyzed the effects of long-term HTP stimulation on gingival epithelial cells using RNA-seq and RRBS. To the best of our knowledge, our study is the first to report a genome-wide analysis of the effects of HTP on gingival epithelial cells. We found that HTP significantly increased *KRT13*, *KLK12*, and *S100A7* expression, which was accompanied by keratinocyte differentiation. GO analysis confirmed that HTP increased the expression of components of the pathways related to keratinocyte differentiation, such as those involved in cornification, keratinization, keratinocyte differentiation, and epithelial differentiation. These results indicate that heated tobacco use may stimulate keratinocyte differentiation in the gingiva. Pathological keratinization,

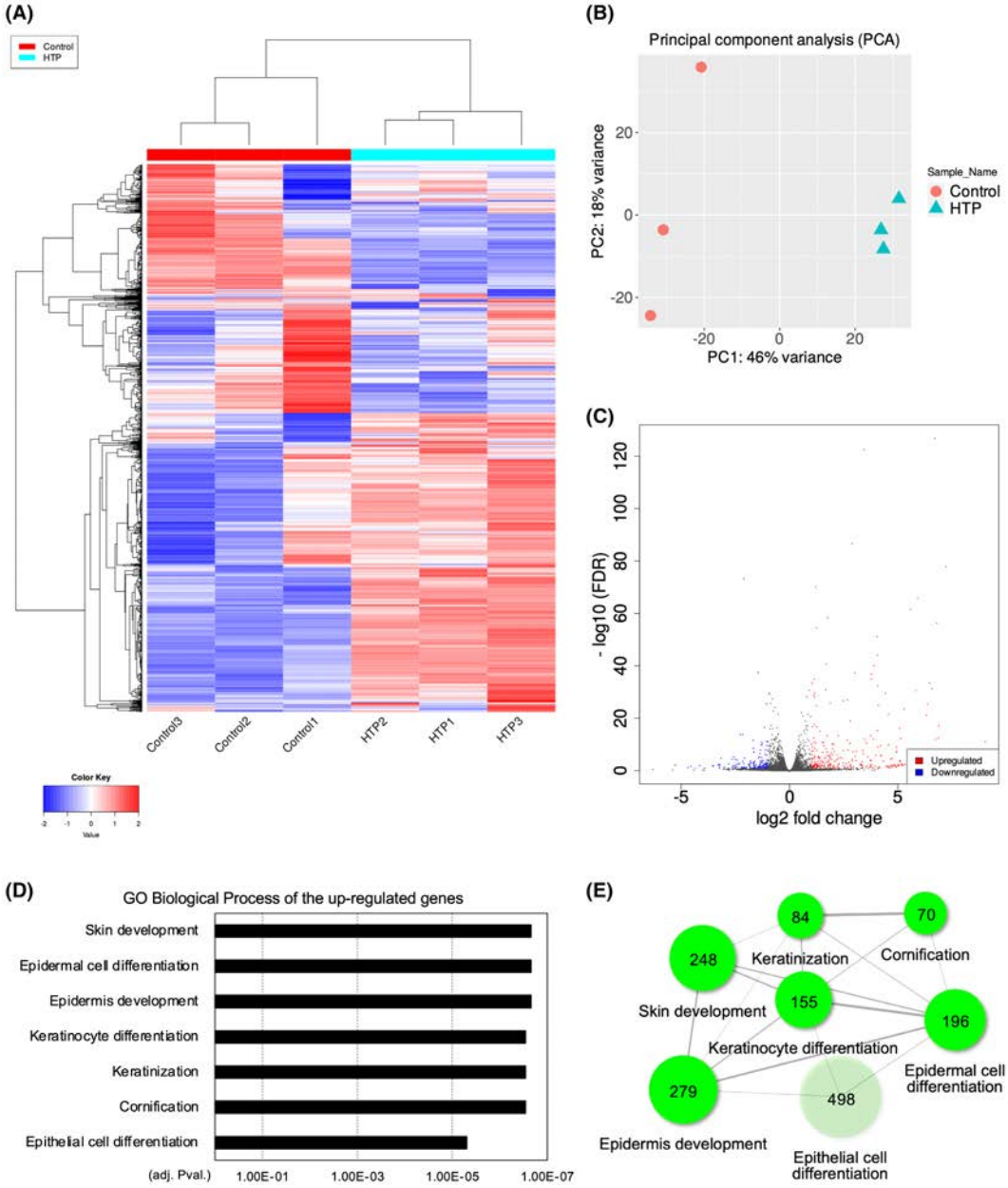

FIGURE 2 Gene expression profiles. (A) Heat map constructed using the most variable genes shows separate hierarchical clustering between the control and heated tobacco product (1% HTP) group samples. (B) Principal component analysis plot shows clear clustering between the control and HTP samples. (C) Volcano plot shows the differentially expressed genes. Compared to the control, the HTP showed higher expression for 284 genes and lower expression for 145 genes (>2-fold change). (D) Gene Ontology analysis (GO) shows that long-term HTP stimulation-induced genes related to cornification, keratinization, epidermis development, epidermal cell differentiation, skin development, keratinocyte differentiation, and epithelial cell differentiation. (E) Network of GO terms and number of related genes in each biological process. This interactive plot also shows the relationship between enriched pathways. Two pathways (nodes) are connected if they share 30% (default, adjustable) or more genes. Green represents downregulated pathways. Darker nodes represent more significantly enriched gene sets. Bigger nodes represent larger gene sets. Thicker edges represent more overlapped genes.

called dyskeratosis, can be observed in tobacco-related oral mucosal diseases, such as leukoplakia, lichen planus, nicotine stomatitis, and squamous cell carcinoma.[15] HTP-stimulated keratinocyte differentiation may thus lead to tobacco-related oral mucosal diseases. Thus, habitual use of Ploom TECH$^+$ may be a risk factor for tobacco-related oral mucosal diseases. Further studies are required to confirm this hypothesis.

Recently, an in vitro study reported the effects of IQOS-heated tobacco on oral keratinocytes and fibroblasts after 24 h. In these experiments, the use of IQOS extracts increased the number of cells in the S and G2/M phases and increased and decreased Bcl2 and p53 expression, respectively. The study suggested that the extract increased oral keratinocyte proliferation.[16] In our study, at 24, 48, and 72 h, HTP treatments did not show higher cell counts than the control

TABLE 2 Up- and down-regulated differentially expressed genes (DEGs) due to the heated tobacco products (top 10).

GeneID	Symbol	Description	log2 Fold Change	Adj. *p* values
Up-regulated differentially expressed genes				
ENSG00000096006	CRISP3	Cysteine rich secretory protein 3	9.038	.000
ENSG00000188505	NCCRP1	NCCRP1, F-Box associated domain containing	7.311	.000
ENSG00000171401	KRT13	Keratin 13	7.226	.000
ENSG00000186474	KLK12	Kallikrein related peptidase 12	7.140	.000
ENSG00000143556	S100A7	S100 calcium binding protein A7	6.992	.000
ENSG00000229732		Novel transcript	6.886	.000
ENSG00000124102	PI3	Peptidase inhibitor 3	6.874	.000
ENSG00000167757	KLK11	Kallikrein related peptidase 11	6.856	.000
ENSG00000136695	IL36RN	Interleukin 36 receptor antagonist	6.810	.000
ENSG00000145879	SPINK7	Serine peptidase inhibitor Kazal type 7	6.794	.000
Down-regulated differentially expressed genes				
ENSG00000186185	KIF18B	Kinesin family member 18B	−5.279	.008
ENSG00000235946	H2BW3P	H2B.W histone 3, pseudogene	−4.553	.025
ENSG00000122420	PTGFR	Prostaglandin F receptor	−4.151	.012
ENSG00000085721	RRN3	RRN3 homolog, RNA polymerase I transcription factor	−3.548	.014
ENSG00000285886		Novel transcript	−3.513	.017
ENSG00000278766		Novel transcript	−3.291	.007
ENSG00000280128		TEC	−3.250	.005
ENSG00000175063	UBE2C	Ubiquitin conjugating enzyme E2 C	−3.206	.007
ENSG00000285833		Novel transcript	−3.162	.000
ENSG00000278311	GGNBP2	Gametogenetin binding protein 2	−3.016	.043

(without HTP) at any concentration. Ploom TECH$^+$ stimulation did not induce cell proliferation. Because the oral mucosa of individuals who use heated tobacco is regularly exposed to the tobacco, we repeatedly stimulated the gingival epithelial cells for 1 month, in accordance with the findings in our previous research.[9] Our experimental design may better reflect habitual cigarette use than the abovementioned study conducted by Pagano et al in 2021.[16]

High levels of KRT13 and KRT4 are expressed in the suprabasal layer of the normal human buccal mucosa, suggesting early differentiation of non-keratinized squamous mucosa.[17] Aberrant KRT13 expression is involved in several pathological conditions. Decreased KRT13 expression has been observed in oral squamous cell carcinoma and dysplasia.[18] KRT13 deficiency was found to cause white sponge nevus.[19] Elevated KRT13 expression might promote tumor metastases.[20,21] In the current study, the upregulated KRT13 expression noted may reflect keratinocyte differentiation or may be related to pathological conditions in gingival epithelial cells. KRT13 upregulation was confirmed at the mRNA level, but no obvious increase was observed at the protein level. Therefore, KRT13 upregulation may not greatly affect gingival epithelial cells.

KLK12 is a type of tissue kallikrein, a subgroup of serine proteases encoding a family of 15 closely related serine proteases.[22] These enzymes are involved in shedding during squamous epithelial desquamation.[21] Many types of kallikreins, including KLK1, KLK4, KLK5, KLK6, KLK7, KLK8, and KLK13, have been detected in skin and keratinocytes,[23] but KLK12 has not been found in keratinocytes. High KLK12 expression might be involved in breast, gastric, and colorectal cancers.[24–27] HTP-induced upregulation of KLK12 expression may be involved in the malignant potential of epithelial cells. However, we detected *KLK12* mRNA, but not protein, indicating that upregulated KLK12 expression did not considerably affect gingival epithelial cells.

S100A7, also known as psoriasin, is highly expressed in patients with psoriasis and other inflammatory diseases. It induces keratinocyte differentiation, resulting in skin and oral epithelial stratification.[28] The involvement of S100A7 in gingivitis and oral squamous cell carcinoma has been reported. Increased S100A7 expression was found in experimentally induced gingivitis.[29] This increased expression may be due to the inflammatory stimulation since IL-1α stimulates the upregulated expression of S100A7 in gingival keratinocytes.[30] In the current study, we observed increased S100A7 expression at both mRNA and protein levels. Therefore, HTP stimulation may increase S100A7 expression resulting from inflammatory changes and keratinocyte differentiation. The involvement of S100A7 in gingivitis and oral squamous cell carcinoma has been reported and has been suggested for use as a diagnostic biomarker.[31,32]

Transcriptional alterations are often caused by genetic methylation in individuals who smoke tobacco.[33] CpG island methylation often affects transcription, and hyper- and hypomethylation directly

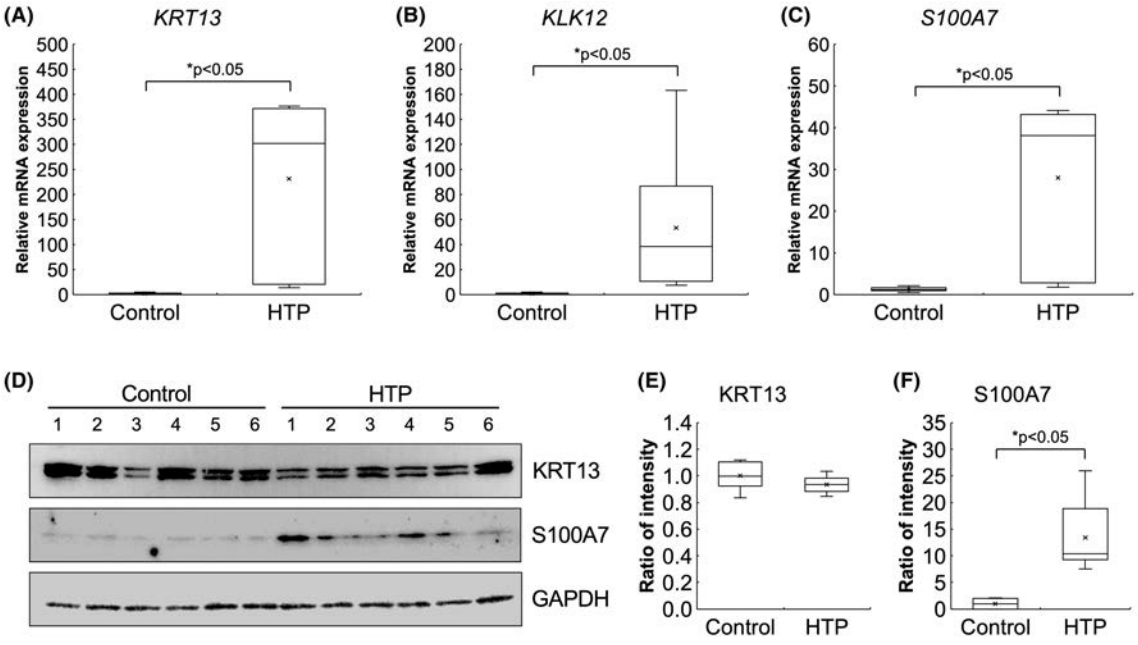

FIGURE 3 Confirmation and reproducibility of data for differentially expressed genes and Gene Ontology biological processes. RNA sequencing (RNA-seq) analysis shows that *KRT13*, *KLK12*, and *S100A7* were upregulated in the heated tobacco product (1% HTP) group and were related to the elevated Gene Ontology terms involving biological processes. (A–C) Quantitative reverse transcriptase PCR confirmed that the *KRT13*, *KLK12*, and *S100A7* mRNA levels with HTP treatment were also significantly higher than those in the control. (D) Western blot results of the S100A7 protein are in accordance with its mRNA expression levels (E, F). Data are presented as the mean ± standard deviation (SD), with a *p*-value of <.05 indicating significance.

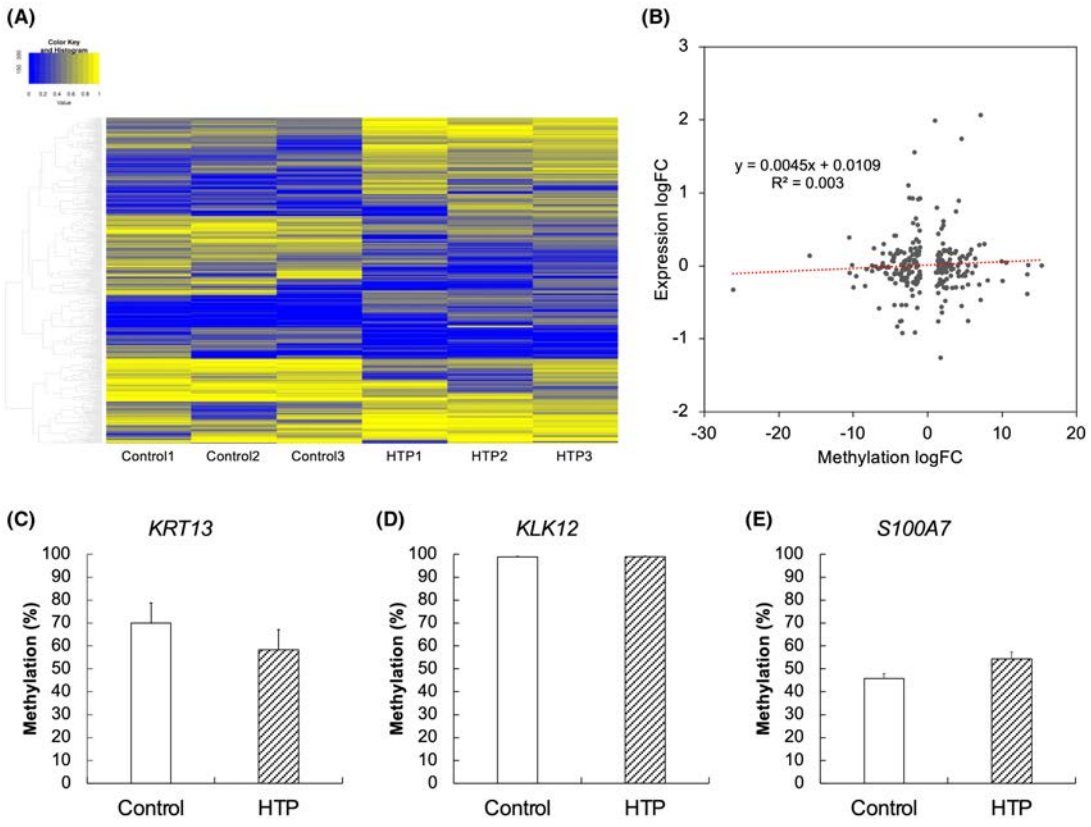

FIGURE 4 Correlation between methylation and gene expression levels. (A) Heat map shows that the methylation levels in the gene promoter region differed between the heated tobacco product (1% HTP) and the control. (B) Scatter plot of methylation levels versus gene expression levels shows that these changes in DNA methylation levels were not correlated with the gene expression levels. (C–E) *KRT13*, *KLK12*, and *S100A7* methylation levels did not show significant alterations. Data are presented as the mean ± SD.

lead to the down- and upregulation of mRNA expression, respectively. Therefore, we examined whether alterations in CpG island methylation were involved in the differential expression of *KRT13*, *KLK12*, and *S100A7*. However, the methylation levels of these genes did not show significant alterations. We performed a global analysis of CpG island methylation with the same experimental models. Although many genes showed hyper- or hypomethylation in HTP-treated samples, a scatter plot of methylation levels versus gene expression levels showed that transcriptional levels were not correlated with methylation levels. Therefore, the overall altered mRNA expression may be unaffected by methylation alterations in HTP-treated samples.

The limitation of this study is that the heated tobacco extracts were crude; therefore, the individual chemicals involved in their effects on gingival epithelial cells are not known. Ploom TECH$^+$ contains many chemical substances such as formaldehyde, acrolein, benzaldehyde, propylene glycol, and glycerol[5]; further research is required to identify the chemicals that exerted the greatest effect on our samples. The crude components may lead to the inhibition of cell growth. Glycerol and propylene glycol are involved in carcinogenesis and may be involved in the dysmorphic and hyperkeratinization of gingival epithelial cells.[34] Moreover, we focused on *KRT13*, *KLK12*, and *S100A7* as upregulated candidate genes in this study. However, it is possible that some other genes may be more effective for oral mucosa.

In conclusion, because long-term HTP stimulation affects epithelial differentiation and keratinization of gingival epithelial cells, habitual Ploom TECH$^+$ use may be a risk factor for tobacco-related oral mucosal diseases. However, the mechanism underlying the induction of epithelial differentiation and keratinization by HTP remains unclear. Our data may aid in further clarifying the disadvantages of heated tobacco use; however, further research is required to confirm this hypothesis.

TABLE 3 Gene ontology (GO) biological processes.

Direction	Pathways	nGenes	Adj. *p* values
Up	Cornification	70	.000
Up	Keratinization	84	.000
Up	Epidermis development	279	.000
Up	Epidermal cell differentiation	196	.000
Up	Skin development	248	.000
Up	Keratinocyte differentiation	155	.000
Up	Epithelial cell differentiation	498	.000

TABLE 4 Hyper- and hypo-methylation of genes (CpG island) due to the heated tobacco products (top 10).

GeneID	Symbol	Description	log2 Fold Change	Adj. *p* values
Hyper-methylation of genes (CpG-island)				
ENSG00000154917	RAB6B	RAB6B, member RAS oncogene family	15.360	.013
ENSG00000178988	MRFAP1L1	Morf4 family associated protein 1 like 1	13.517	.001
ENSG00000139970	RTN1	Reticulon 1	13.400	.042
ENSG00000180190	TDRP	Testis development related protein	13.380	.000
ENSG00000179051	RCC2	Regulator of chromosome condensation 2	10.571	.015
ENSG00000198915	RASGEF1A	RasGEF Domain Family Member 1A	10.098	.000
ENSG00000095485	CWF19L1	CWF19 like cell cycle control factor 1	9.928	.000
ENSG00000042286	AIFM2	Apoptosis inducing factor mitochondria associated 2	8.086	.000
ENSG00000101166	PRELID3B	PRELI domain containing 3B	7.648	.000
ENSG00000059145	UNKL	Unk like Zinc finger	7.163	.000
Hypo-methylation of genes (CpG-island)				
ENSG00000137075	RNF38	Ring finger protein 38	−26.144	.000
ENSG00000136816	TOR1B	Torsin family 1 member B	−15.824	.000
ENSG00000171219	CDC42BPG	CDC42 binding protein kinase gamma	−10.524	.020
ENSG00000196391	ZNF774	Zinc finger protein 774	−10.473	.000
ENSG00000106638	TBL2	Transducin Beta Like 2	−10.138	.010
ENSG00000101004	NINL	Ninein Like	−9.935	.001
ENSG00000253716	MINCR	MYC-Induced long non-coding RNA	−9.565	.017
ENSG00000164976	MYORG	Myogenesis regulating glycosidase (Putative)	−8.380	.000
ENSG00000269556	TMEM185A	Transmembrane protein 185A	−8.209	.012
ENSG00000187051	RPS19BP1	Ribosomal protein S19 binding protein 1	−7.451	.000

AUTHOR CONTRIBUTIONS

OU, NN, DH, and YA designed the study. OU, NN, DH, DP, NS, TM, KY, and YK collected and analyzed the data. OU, NN, DH, YK, TS, YF, HM, and YA interpreted the data. OU, NN, DH, DP, YK, and YA drafted and revised the manuscript. All authors have approved this manuscript for submission.

ACKNOWLEDGEMENTS

We would like to thank Editage (www.editage.com) for English language editing.

FUNDING INFORMATION

This research was supported by the Uehara Memorial Foundation, JSPS KAKENHI Grant Number JP22K17213, and Advanced Research Promotion Center, Health Sciences University of Hokkaido.

CONFLICT OF INTEREST STATEMENT

The authors declare no conflict of interest.

DATA AVAILABILITY STATEMENT

The data that support the findings of this study are available from the corresponding author upon reasonable request.

ORCID

Osamu Uehara https://orcid.org/0000-0001-5602-4448
Koki Yoshida https://orcid.org/0000-0002-3792-9011
Yutaka Kawano https://orcid.org/0000-0002-2256-0776
Yoshihiro Abiko https://orcid.org/0000-0001-6358-8508

REFERENCES

1. Zhang Y, He J, He B, Huang R, Li M. Effect of tobacco on periodontal disease and oral cancer. *Tob Induc Dis*. 2019;17:40.
2. Leigh NJ, Tran PL, O'Connor RJ, Goniewicz ML. Cytotoxic effects of heated tobacco products (HTP) on human bronchial epithelial cells. *Tob Control*. 2018;27(suppl 1):s26-s29.
3. St Helen G, Jacob P III, Nardone N, Benowitz NL. IQOS: examination of Philip Morris International's claim of reduced exposure. *Tob Control*. 2018;27(Suppl 1):s30-s36.
4. Forster M, Fiebelkorn S, Yurteri C, et al. Assessment of novel tobacco heating product THP1.0. Part 3: comprehensive chemical characterisation of harmful and potentially harmful aerosol emissions. *Regul Toxicol Pharmacol*. 2018;93:14-33.
5. Uchiyama S, Noguchi M, Takagi N, et al. Simple determination of gaseous and particulate compounds generated from heated tobacco products. *Chem Res Toxicol*. 2018;31:585-593.
6. Aokage T, Tsukahara K, Fukuda Y, et al. Heat-not-burn cigarettes induce fulminant acute eosinophilic pneumonia requiring extracorporeal membrane oxygenation. *Respir Med Case Rep*. 2019;26:87-90.
7. Znyk M, Jurewicz J, Kaleta D. Exposure to heated tobacco products and adverse health effects, a systematic review. *Int J Environ Res Public Health*. 2021;18:6651.
8. Uehara O, Takimoto K, Morikawa T, et al. Upregulated expression of MMP-9 in gingival epithelial cells induced by prolonged stimulation with arecoline. *Oncol Lett*. 2017;14:1186-1192.
9. Kimura I. *Harmful Effects of Smoking on Neurovascular Unit*. Fukuoka University; 2019:31 Dissertation (published in Japanese).
10. Ge SX, Son EW, Yao R. iDEP: an integrated web application for differential expression and pathway analysis of RNA-Seq data. *BMC Bioinform*. 2018;19:534.
11. Livak KJ, Schmittgen TD. Analysis of relative gene expression data using real-time quantitative PCR and the $2^{-\Delta\Delta CT}$ method. *Methods*. 2001;25:402-408.
12. Lu L, Katsaros D, de la Longrais IAR, Sochirca O, Yu H. Hypermethylation of let-7a-3 in epithelial ovarian cancer is associated with low insulin-like growth factor-II expression and favorable prognosis. *Cancer Res*. 2007;67:10117-10122.
13. Chen Y, Pal B, Visvader JE, Smyth GK. Differential methylation analysis of reduced representation bisulfite sequencing experiments using edgeR. *F1000Res*. 2017;6:2055.
14. Rodríguez-Paredes M, Esteller M. Cancer epigenetics reaches mainstream oncology. *Nat Med*. 2011;17:330-339.
15. Woo SB. Oral epithelial dysplasia and premalignancy. *Head Neck Pathol*. 2019;13:423-439.
16. Pagano S, Negri P, Coniglio M, et al. Heat-not-burn tobacco (IQOS), oral fibroblasts and keratinocytes: cytotoxicity, morphological analysis, apoptosis and cellular cycle. An in vitro study. *J Periodontal Res*. 2021;56:917-928.
17. Ponniah G, Rollenhagen C, Bahn Y-S, Staab JF, Sundstrom P. State of differentiation defines buccal epithelial cell affinity for cross-linking to *Candida albicans* Hwp1. *J Oral Pathol Med*. 2007;36:456-467.
18. Sakamoto K, Aragaki T, Morita K, et al. Down-regulation of keratin 4 and keratin 13 expression in oral squamous cell carcinoma and epithelial dysplasia: a clue for histopathogenesis. *Histopathology*. 2011;58:531-542.
19. Simonson L, Vold S, Mowers C, et al. Keratin 13 deficiency causes white sponge nevus in mice. *Dev Biol*. 2020;468:146-153.
20. Yin L, Li Q, Mrdenovic S, et al. KRT13 promotes stemness and drives metastasis in breast cancer through a plakoglobin/c-Myc signaling pathway. *Breast Cancer Res*. 2022;24:7.
21. Li Q, Yin L, Jones LW, et al. Keratin 13 expression reprograms bone and brain metastases of human prostate cancer cells. *Oncotarget*. 2016;7:84645-84657.
22. Kalinska M, Meyer-Hoffert U, Kantyka T, Potempa J. Kallikreins–the melting pot of activity and function. *Biochimie*. 2016;122:270-282.
23. Komatsu N, Takata M, Otsuki N, et al. Expression and localization of tissue kallikrein mRNAs in human epidermis and appendages. *J Invest Dermatol*. 2003;121:542-549.
24. Yousef GM, Magklara A, Diamandis EP. KLK12 is a novel serine protease and a new member of the human kallikrein gene family-differential expression in breast cancer. *Genomics*. 2000;69:331-341.
25. Zhao E-H, Shen Z-Y, Liu H, Jin X, Cao H. Clinical significance of human kallikrein 12 gene expression in gastric cancer. *World J Gastroenterol*. 2012;18:6597-6604.
26. Li Q, Zhou X, Fang Z, Zhou H. Knockdown of KLK12 inhibits viability and induces apoptosis in human colorectal cancer HT-29 cell line. *Int J Mol Med*. 2019;44:1667-1676.
27. Li LQ, Li J, Chen Y, Lu YF, Lu LM. De novo transcriptome analysis of tobacco seedlings and identification of the early response gene network under low-potassium stress. *Genet Mol Res*. 2016;15:gmr.15038599.
28. Wagner T, Beer L, Gschwandtner M, et al. The differentiation-associated keratinocyte protein cornifelin contributes to cell-cell adhesion of epidermal and mucosal keratinocytes. *J Invest Dermatol*. 2019;139:2292-2301.e9.
29. Dommisch H, Staufenbiel I, Schulze K, et al. Expression of antimicrobial peptides and interleukin-8 during early stages of inflammation: an experimental gingivitis study. *J Periodontal Res*. 2015;50:836-845.

30. Hiroshima Y, Bando M, Kataoka M, et al. Regulation of antimicrobial peptide expression in human gingival keratinocytes by interleukin-1α. *Arch Oral Biol*. 2011;56:761-767.
31. Fukuzawa H, Kiyoshima T, Kobayashi I, Ozeki S, Sakai H. Transcription promoter activity of the human S100A7 gene in oral squamous cell carcinoma cell lines. *Biochim Biophys Acta*. 2006;1759:171-176.
32. Sood A, Mishra D, Kharbanda OP, et al. Role of S100 A7 as a diagnostic biomarker in oral potentially malignant disorders and oral cancer. *J Oral Maxillofac Pathol*. 2022;26:166-172.
33. Zong D, Liu X, Li J, Ouyang R, Chen P. The role of cigarette smoke-induced epigenetic alterations in inflammation. *Epigenetics Chromatin*. 2019;12:65.
34. Tarran R, Barr RG, Benowitz NL, et al. E-cigarettes and cardiopulmonary health. *Function (Oxf)*. 2021;2:zqab004.

How to cite this article: Uehara O, Nakamoto N, Hiraki D, et al. Effects of prolonged stimulation with heated tobacco products (Ploom TECH^{+}) on gingival epithelial cells. *J Periodont Res*. 2023;00:1-11. doi:10.1111/jre.13123